15

Robust Control of Sensorless AC Drives Based on Adaptive Identification

Birou M.T. Iulian
Technical University of Cluj-Napcoa, Department of Electrical Drives and Robots
Romania

1. Introduction

In most of the modern drive systems with alternating current (AC) machines which require rotor speed control, the main task is to design and develop different controllers, able to achieve high dynamic performance and to maintain the system response within specified tolerances, for a wide range of speed and torque values, for parameter variations and for external perturbations like: total inertia moment, friction coefficient, etc. (Leonhard, 1985). Various concepts for controlled AC drives without speed sensor (sensorless control) have been developed in the past few years (Holtz, 2002; Rajashekara et al., 1996; Vas, 1998). Ongoing research has focused on providing sustained operation at high dynamic performance at very low speed, including zero speed and zero stator frequency (Akatsu & Kawamura, 2000; Holtz & Quan, 2002; Hurst et al., 1998; Lascu et al., 2005). In speed sensorless control, motor parameter sensitivity is an important and large discussed and analyzed problem (Akpolat et al., 2000; Toliyat et al., 2003). In many existing speed identification algorithms, the rotor speed is estimated based on the rotor flux observer. Therefore, these algorithms are, to a certain degree, machine parameter dependent. The solution proposed in this chapter is to apply robust control to sensorless AC drive systems.
The designing procedure of the speed controllers can be very difficult, if a complex mathematical model of the plant (here of the AC machine) is used. But robust controllers keep the dynamic and stability performance of the controlled system even if structured or unstructured uncertainties appear. That's why, robust speed controllers can be designed by using simplified models of the AC machines, and have to be used in a complex structure based on the field-oriented control (FOC) principle (Birou & Pavel, 2008). Thus, the requirements of a digital control application are: a flexible control structure, reduced hardware configuration and a good dynamic behavior of the controlled process. The last two aspects can be realized by finding a compromise between the reducing of the control cycle times and the increasing of controller complexity. For industrial applications the hardware costs are also important.
Two different algorithms will be presented to estimate the rotor speed in this chapter, one based on the model reference adaptive system (MRAS) and the other on a full order observer (FOO). The speed identification algorithms, the designing procedure of the optimal H_∞ controller and the robust control of the sensorless driving system will be accomplished by simulated and experimental results. Based on the results obtained, advantages and disadvantages of the proposed control structures will be discussed.

2. Control of AC machines

Electrical machines are the major and most efficient source to generate motion for a large number of applications in a wide range of power (from μW to several hundred of MW). Among all types of electromechanical converters, the AC machines are now, from fare, the most produced and used in variable speed applications, because of their high performance/cost ratio. If for low power applications (i.e. servo drives), generally permanent magnet synchronous machines (PM-SM) and for very high powers electrical excited synchronous machines (SM) are used, the largest number of applications use rotor cage induction machines (IM) because of their higher mechanical robustness and lower cost (Birou et al., 2010; Holtz, 2002; Kelemen & Imecs, 1991; Leonhard, 1985; Moreira et al., 1991; Wieser, 1998; Trzynadlowski, 1994). The main disadvantage of using in the past the IM as motion source in variable speed applications, namely the difficulty to precisely control speed and/or torque, is now compensate by using:

- power electronics in wide power range (voltage-source or current-source converters), to fed AC machines with variable amplitude/frequency power signals (voltage or current);
- modern control methods, like field oriented based vector control (VC) or direct torque control (DTC) strategies of AC drive systems;
- high frequency, real-time, digital computing systems, based on microcontrollers (μC) or digital signal processors (DSP), able to implement an perform the designed strategies and control methods.

Depending on the dynamic performances, energy efficiency demands and final cost of the electrical drive system, following control strategies can be used:

- scalar control (SC) of AC machines, considering the two torque producing components of the electrical machine (the current and the electromagnetic flux) only as scalar variables, without information about their phasorial positions. The current, speed or position control loops are able to impose good enough dynamic performances for a large number of applications;
- vector control (VC) of AC machines, based on the field-oriented control (FOC) principle, where the motion control loop (position, speed or torque loop) and the magnetizing control loop (flux loop) are decoupled by using the flux phasor (vector) as reference system and splitting the current phasor into an active and a reactive component. This control strategy is the most computer time and effort demanding (revealed also in the costs of the system) but ensure the best dynamic performances and energy efficiency in variable speed control;
- direct torque control (DTC) of AC machines, used widely in variable torque applications like electric traction systems, based on the direct control of the torque producing current, considering the limited number of possible topologic configurations of one of the power converter components, namely the pulse width modulated (PWM) inverter.

In the designing procedure of the controllers, it is important to know the transfer function of the process. A transfer function which describes exactly the behavior of the AC machine is almost impossible to obtain, because of the nonlinearities of the mathematical model of the machine. Consequently a simplified transfer function of the process is used to design the speed controller. Then, the control law is introduced in the not simplified and nonlinear "original" control structure, in order to simulate and analyze the dynamic behavior of the

mechanical and electrical variables (speed, torque, currents, voltages, etc.). In our drive system, the simplified transfer function describes the linear model of the AC machine corresponding to a steady state working point and is presented in Fig. 1. A vector control strategy will be applied to control the variable speed electrical drive systems discussed in this chapter. For the proposed FOC of the AC machine, the rotor flux vector is considered to be the reference system. In this case the speed controller has as input the speed error Δn_r and computes the control variable as the active component of the stator current $i^*_{\text{Active}}=i_{sq\lambda r}$, as described by Equation 1.

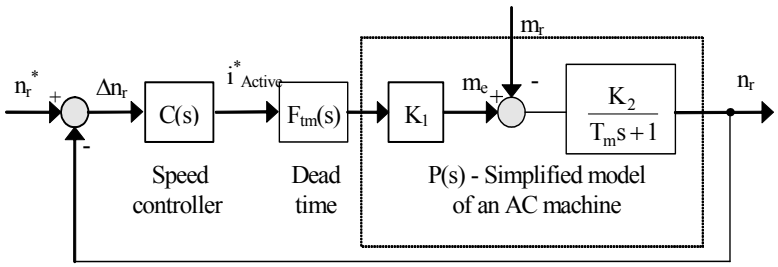

Fig. 1. Simplified speed close-loop control structure of an ac machine.

Using the torque producing expression:

$$m_e = \frac{3}{2} z_p \frac{L_m}{L_r} \Im m\left(\underline{i}_s \underline{\Psi}_r^*\right) = \frac{3}{2} z_p \frac{L_m}{L_r} \Psi_r i_{sq\lambda_r}, \tag{1}$$

with L_m and L_r the magnetic (mutual) and rotor inductance respectively, z_p the number of pole pairs and the motion equation

$$m_e = Js\omega_r + B\omega_r + m_r, \tag{2}$$

where J is the total moment of inertia, B the friction coefficient, s the derivate symbol and ω_r the rotor angular velocity

$$\omega_r = \frac{\omega}{z_p} = n_r \frac{2\pi}{60}, \tag{3}$$

with ω the electrical angular velocity and n_r the rotor speed. The simplified transfer function of the rotor-flux oriented AC machine can be written:

$$P(s) = \frac{n_r}{i^*_{sq\lambda r}} = K_1 \frac{K_2}{T_m s + 1} = \frac{K_m}{T_m s + 1}. \tag{4}$$

If we apply to the speed control loop presented in Fig. 1 the module criteria and consider the non compensable component described by the dead-time transfer function:

$$F_{t.m}(s) = e^{-\tau_m s}, \tag{5}$$

the speed controller will have a transfer function as follows:

$$C_{PI}(s) = K_P \cdot \left(1 + \frac{1}{T_i s}\right). \tag{6}$$

It results a classical PI controller, having K_p - the proportional coefficient and $K_i = K_p / T_i$ - the integrator coefficient. Considering the two first-order integrator type transfer functions of the direct loop having constant times of different ranges, with $\tau_m << T_m$,

$$K_m e^{-(\tau_m + T_m)s} \cong K_m e^{-T_m s}, \tag{7}$$

the equivalent closed-loop transfer function of Fig.1 becomes:

$$H_o(s) = \frac{K_P K_m (1 + T_i s)}{T_i s(T_m s + 1) + K_P K_m (1 + T_i s)} \tag{8}$$

3. Sensorless control of AC machines based on adaptive identification

The common accepted definition of sensorless control for electrical drives means the need of speed and/or torque control of an electrical machine without using any mechanical speed or position measuring device placed on the rotor ax. Recently, sensorless control of AC drives is a prolific research area and many viable solutions have been proposed and implemented. It combines favorably the cost advantage with increased reliability due to the absence of the mechanical sensor and its communication cable. Speed sensorless AC drives are today well established in industrial applications where no persistent operation at lower speed occurs.
The main philosophy in sensorless control is to use the electrical machine itself as a "sensor" by offering the necessary information able to estimate its position or speed (Consoli et al., 2003; Lorenz 2010). Several techniques have been developed and published in application with both FOC and DTC of AC drives. A first category comprises signal injection techniques, based on spectral analysis which use either the natural (if it exists), or an artificial created, anisotropy of the magnetic field of the AC machine (Briz et al., 2004; Degner & Lorenz, 2000; Holtz 2006; Kim & Lorenz, 2004). By injecting appropriate voltage signals in the stator (mainly high frequency signals) and analyzing the obtained current or voltage harmonics, valuable information can be extracted to determine the rotor position. A second category comprises techniques which estimate the rotor position/speed starting from the real process (drive system) and from the mathematical model of the machine by using different identification algorithms, like:

- open-loop state estimation using simple models and improved schemes with compensation of nonlinearities and disturbances (Holtz & Quan, 2002);
- model reference adaptive system based techniques (Birou & Pavel, 2008; Cirrincione & Pucci, 2005; Landau, 1979; Lascu et al., 2005);
- adaptive and robust observer (mainly Kalman filter or Lueneberger observers) based on fundamental excitation and advanced models (Caruana et al., 2003; Hinkkanen, 2004; Jansen et al., 1994);
- estimators using artificial intelligence, in particular fuzzy-logic systems, neural networks and genetic algorithms (Zadeh, 1996) .

The proposed solution is based on a FOC structure with AC machine, using for speed estimation a model reference adaptive system (MRAS) algorithm and a full order observer (FOO) respectively, like presented in Fig. 2.

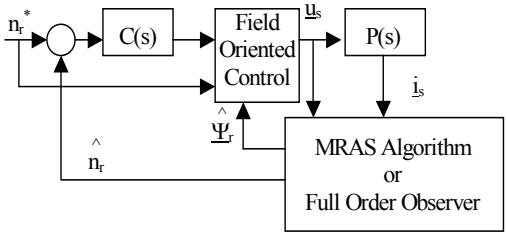

Fig. 2. Block diagram of the speed sensorless vector control of the induction machine

3.1 Model reference adaptive system algorithm for speed identification

In order to achieve sensorless control, the rotor speed estimation has to be indirectly derived based on the measured stator voltages and currents. Therefore, a mathematical model of the induction machine is needed. The model is described in the stationary (stator) reference frame. The block diagram of the MRAS speed identification is shown in Fig. 3. It contains a reference model, an adjustable model and an adaptive algorithm. Both models have as inputs the stator voltages and currents. The reference model outputs a performance index p and the adjustable model a performance index $\hat{p}$. The difference between the two values is used by the adaptive algorithm to converge the estimated speed $\hat{\omega}$ to its real value.

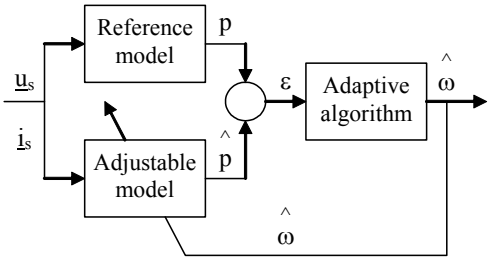

Fig. 3. Model reference adaptive system algorithm (MRAS) for speed identification.

In order to estimate the rotor speed accurately, the performance index of the reference model has to be robust over the entire speed range and insensitive to the machine parameters. According to the equations of the induction machine, we can obtain the value of the rotor flux phasor based on stator equations:

$$\frac{d\underline{\Psi}_r}{dt} = \frac{L_r}{L_m}\left(\underline{u}_s - R_s\underline{i}_s - L_\sigma\frac{d\underline{i}_s}{dt}\right), \tag{9}$$

where L_σ is the equivalent inductance and R_s is the stator resistance. The same rotor flux phasor based on the rotor equations:

$$\frac{d\underline{\Psi}_r}{dt} = -\frac{1}{\tau_r}\underline{\Psi}_r + j\omega\underline{\Psi}_r + \frac{L_m}{\tau_r}\underline{i}_s\,, \tag{10}$$

where $\tau_r = L_r / R_r$ is the rotor time constant. Considering the electromotive induced voltage (back EMF) being:

$$\underline{e} = \frac{L_m}{L_r}\frac{d\underline{\Psi}_r}{dt} \tag{11}$$

and decoupling Equation 9 on the stationary (stator-fixed) reference frame *d-q*, we obtain:

$$e_d = u_{sd} - R_s i_{sd} - L_\sigma \frac{di_{sd}}{dt}\,, \tag{12}$$

$$e_q = u_{sq} - R_s i_{sq} - L_\sigma \frac{di_{sq}}{dt}\,. \tag{13}$$

Considering a formal magnetizing current

$$\underline{i}_m = \frac{1}{L_m}\underline{\Psi}_r \tag{14}$$

and decupling Equation 10 on the fix reference frame *d-q*, we have:

$$e_{md} = -\frac{L_m^{\,2}}{L_r}\left(\frac{1}{\tau_r}i_{md} + \omega i_{mq} - \frac{1}{\tau_r}i_{sd}\right), \tag{15}$$

$$e_{mq} = -\frac{L_m^{\,2}}{L_r}\left(\frac{1}{\tau_r}i_{mq} - \omega i_{md} - \frac{1}{\tau_r}i_{sq}\right). \tag{16}$$

The reference model is described based on Equations 12 and 13 and is parameter dependent, namely with the stator resistance R_s and the equivalent inductance L_σ. In the reference model there are no integral operations, so the model can be used also for low speed estimation. To improve the robustness of the reference model, one of the two machine parameters can be avoided by choosing an optimal way to define the reference model performance index *p*. To eliminate the effect of the inductance L_σ, Equations 12 and 13 are cross multiplied by the derivates of the two stator current components and we obtain:

$$p = u_{sd}\frac{di_{sq}}{dt} - u_{sq}\frac{di_{sd}}{dt} - R_s\left(i_{sd}\frac{di_{sq}}{dt} - i_{sq}\frac{di_{sd}}{dt}\right). \tag{17}$$

Equation 17 describes the performance index of the reference model. To obtain the performance index of the adjustable model, same mathematical operations applied to Equations 15 and 16 give:

$$\hat{p} = \frac{L_m^2}{L_r}\frac{1}{\tau_r}\left(i_{sd}\frac{di_{sq}}{dt} - i_{sq}\frac{di_{sd}}{dt}\right) - \frac{L_m^2}{L_r}\frac{1}{\tau_r}\left(i_{md}\frac{di_{sq}}{dt} - i_{mq}\frac{di_{sd}}{dt}\right) - \frac{L_m^2}{L_r}\hat{\omega}\left(i_{mq}\frac{di_{sq}}{dt} - i_{md}\frac{di_{sd}}{dt}\right) \quad (18)$$

having the two formal magnetizing current components described by:

$$\frac{di_{md}}{dt} = -\frac{1}{\tau_r}i_{md} - \hat{\omega}i_{mq} + \frac{1}{\tau_r}i_{sd}\,, \quad (19)$$

$$\frac{di_{mq}}{dt} = -\frac{1}{\tau_r}i_{mq} + \hat{\omega}i_{md} + \frac{1}{\tau_r}i_{sq}\,. \quad (20)$$

Equation 17 is used for the reference model and Equation 18 for the adjustable model. The error between the two performance indexes

$$\varepsilon = p - \hat{p} \quad (21)$$

is the input for the adaptive algorithm, see Fig. 3. This algorithm estimates the $\hat{\omega}$ rotor speed in order to converge the performance index of the adjustable model to the performance index of the reference model (converge the error ε to zero). In designing the adaptive mechanism of the presented MRAS structure, it is necessary to ensure the stability of the control system and the convergence of the estimated speed to the real one. Based on the hyper-stability theory (Landau, 1979), following adaptive mechanism is used in order to guarantee the system stability:

$$\hat{\omega} = K_p\varepsilon + K_i\int\varepsilon dt\,, \quad (22)$$

where, K_p and K_i are the gain parameters of the adaptive algorithm, limited only by noise considerations and having for our control structure the particular values K_p=3 and K_i=10. The MRAS algorithm presented above can also be used for on-line identification of some parameter of the induction machine, namely the stator resistance, the equivalent inductance or the rotor time constant.

3.2 Speed and rotor flux estimator based on a full order observer

The speed estimation strategy with full order observer (FOO) is based on the fundamental excitation variables as information source, like presented in Fig. 4. The rotor speed estimator is based on comparing the stator current estimate value $\hat{i}_s$ to the actual stator current i_s and updating the estimated speed $\hat{\omega}$ such that the error i_s- $\hat{i}_s$ is minimized in some sense. This will be done by using a full-order observer for the estimated stator current, rotor flux and rotor speed, described by equations:

$$L_\sigma\frac{d\hat{\underline{i}}_s}{dt} = \underline{u}_s - \left(R_s + R_r + j\omega_\lambda L_\sigma\right)\hat{\underline{i}}_s + \left(\frac{R_r}{L_m} - j\omega\hat{}\right)\hat{\underline{\Psi}}_r + k_1\left(\underline{i}_s - \hat{\underline{i}}_s\right), \quad (23)$$

$$\frac{d\hat{\underline{\Psi}}_r}{dt} = R_r \hat{\underline{i}}_s - \left[\frac{R_r}{L_m} + j\left(\omega_\lambda - \hat{\omega}\right)\right]\hat{\underline{\Psi}}_r + k_2\left(\underline{i}_s - \hat{\underline{i}}_s\right), \tag{24}$$

$$\frac{d\hat{\omega}}{dt} = \Re e\left\{k_3\left(\underline{i}_s - \hat{\underline{i}}_s\right)\right\}, \tag{25}$$

where ω_λ is the speed of the reference frame and k_1, k_2 and k_3 are the gain parameters of the algorithm, calculated from the Ricatti equation.

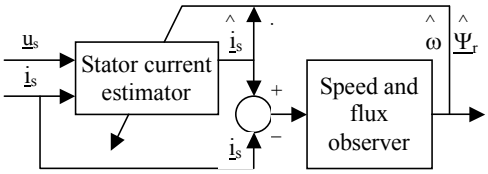

Fig. 4. Full order observer (FOO), for speed and rotor flux estimation

The speed estimator must converge significantly faster than the mechanical speed control loop in order to ensure good tracking. So, the dynamics of the speed estimator can be neglected as seen from the much slower flux and speed dynamics and thus it can be considered only that value of estimated speed and stator current which have converged to quasi steady-state values. The control structure based on the MRAS algorithm presented in 3.1 will be implemented on a driving system, composed of an induction machine with the following main catalog values:

- rated power P_N 2,2 *kW*,
- rated speed n_N 1435 rpm.,
- nominal stator current I_{sN} 4,9 *A*,
- rated stator voltage U_{sN} 400*V*,
- nominal load torque M_N 14,7 *Nm*.

Simulated results of the MRAS algorithm are presented in Fig. 5, where the reference model performance index p, the adjustable model performance index $\hat{p}$ (Equations 17 and 18), and error ε (Equation 21) are for a starting process to the rated speed with rated load torque.

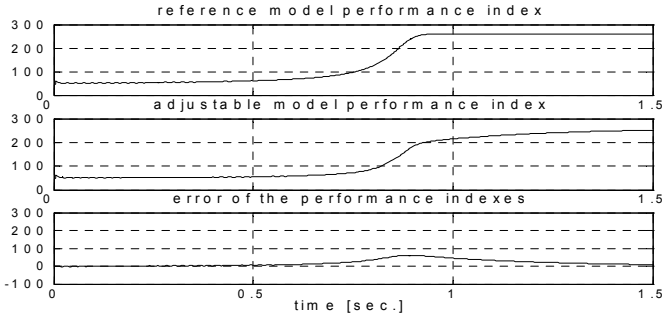

Fig. 5. The performance index of reference model p, adjustable model $\hat{p}$ and error index ε.

The simulated speed of this process, the estimated speed based on the MRAS algorithm and the speed error estimation are presented in Fig. 6. Problems that may occur by derivation of the measured stator currents can be avoided using specific digital algorithms.

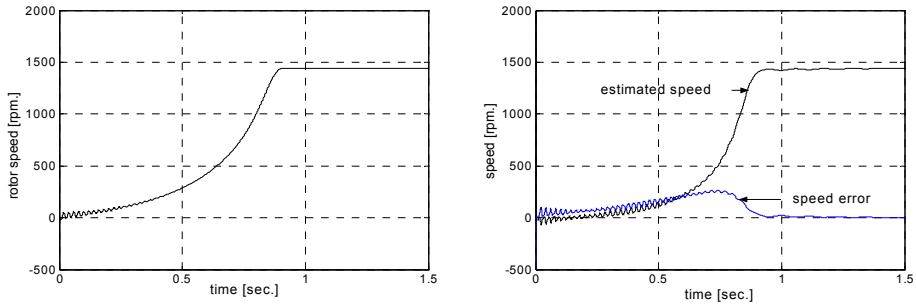

Fig. 6. Rotor speed, estimated speed based on the MRAS algorithm and speed error for a starting process at rated speed with rated torque.

Simulated results confirm that the advantage of using the MRAS algorithm, for the control of a sensorless driving system, is a high dynamic performance at speed and torque steps. The error of the estimated speed in the starting process is relative big, because of the sensitivity of the control structure with speed estimators to parameter variations (rotor time constant) and external perturbations (moment of inertia, friction coefficient). By modifying the gain parameters from Equation 22 we can avoid this, but we disturb the control performance parameters (overshooting, stationary error). So, increasing robustness of the sensorless control is needed. The proposed solution is to apply the robust control theory to the AC drive, by designing an optimal H_∞ controller, to ensure the stability and robustness performances of the driving system.

4. Robust control of AC drives

A control system is considered to be robust if it is insensitive to internal process parameter variations or external perturbations (McFarlene & Glover, 1990; Safonov, 1980). In driving systems with AC machines, the most sensible elements are:

- rotor resistance or rotor time constant because of their strong variation due to the inner temperature of the machine and because of their influence in the machine model;
- mutual inductance (magnetic inductance) because of his nonlinearity (saturation effect);
- total inertia moment of the system with possible nonlinear or even random variations (especially by robot arms);
- load torque for a wide range of applications.

The main goal of a robust controller is to compensate the effects introduced by the variations of the sensitive elements described above to the dynamic process of the controlled system

The designing process of a robust controller may follow different methods, applying various robust control system synthesis techniques (Ball & Helton, 1993; Chiang & Safonov, 1992; Doyle et al., 1989; Morari & Zafiriou, 1990; Zames, 1996). The main methods are based on geometric-analytical, frequency domain or steady-state approaches like: Hardy space based,

optimal H_2 and H_∞ techniques (Green & Limebeer, 1995; Ionescu et al., 1998; Kwakernaak, 1993; Mita et al., 1998), linear quadratic optimal LQG (Kucera, 1993), LQG/LTR (Doyle et al., 1989) or LQR (Chiang & Safonov, 1992) techniques and square root based μ synthesis techniques (Apkarian & Morris, 1993). An optimal H_∞ technique will be used in this chapter for the robust control of the driving system because of the relative simple designing process of the controller and the high robust performances obtained (Bryson, 1996). The designing procedure for the optimal controller will start by describing the driving system with AC machine in steady state equations as a linear multivariable system.

4.1 Mathematical model of the real driving system with AC machine

Fig. 1 presents the closed loop control system of an AC drive. The controlled process is described by a simplified model $P(s)$ of the AC machine (valuable for both the induction and the synchronous machine). The robust control problem is to design an optimal speed controller $C(s)$ able to satisfy the robust-stability and robust-performance criteria of the controlled system. The difference between the real physical system (in our case the AC driving system) and his mathematical model, difference defined as mathematical uncertainty may have several causes, namely:

- the AC driving system (like most of the real systems) is nonlinear, while the mathematical model is linear around a static working point, so the model exactly describes the process only around this working point;
- simplification constrains in modeling the process (AC machine in our case) based on high number of variables and parameter involved;
- process parameter variations and external perturbations are difficult to be exactly modeled;
- dynamic behavior of the driving system can not be exactly modeled.

The mathematical uncertainties can be structural uncertainties, based on parameter variations of the dynamic process like rotor time constant and nonstructural uncertainties, frequency dependent like magnetic saturation or external perturbations (moment of inertia, load torque). The study of system robustness based on the H_∞ control theory is based on describing the model uncertainty as transfer function (matrix) different from the nominal one. The most used methods to describe them are like additive uncertainties, multiplicative uncertainties or a superposition of both uncertainties, like presented in Fig. 7. Using them, the real process can be written based on the modeled one (nominal plant) as:

$$P(s) = P_N(s) + \Delta_A(s) \tag{26}$$

in the case of additive uncertainties, and :

$$P(s) = (I + \Delta_M(s))P_N(s) \tag{27}$$

in the case of multiplicative uncertainties, where $P_N(s)$ is the nominal (rated) plant, $P(s)$ is the real plant (perturbed process), $\Delta_A(s)$ is the additive uncertainty and $\Delta_M(s)$ is the multiplicative uncertainty. Analyzing the dynamic behavior of the process in frequency domain by using additive or multiplicative uncertainties, the model will describe better the real system in stationary frame or at lower frequencies and the uncertainties will increase at higher frequencies.

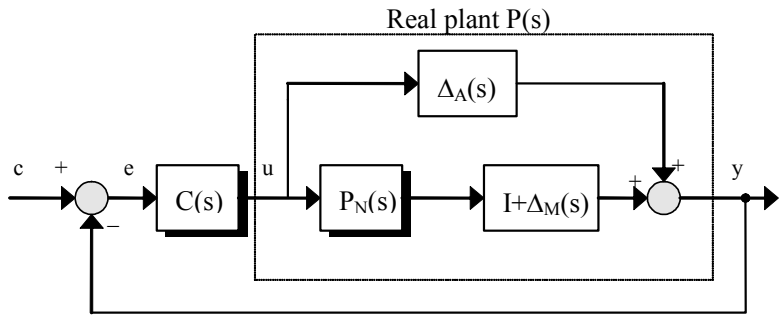

Fig. 7. Diagram of the controlled process using the additive and multiplicative uncertainty.

4.2 Optimal H_∞ controller design for the driving system

The extended H_∞ control theory is used to design a robust speed-control solution for AC driving systems. It has to satisfy the robust stability characteristics of the control structure as well as the dynamic performances of the driving system. Considering a Laplace transform matrix $G(s) \in C^{mxn}$ of a multivariable system with n inputs and m outputs and $\bar{\sigma}(G)$ the greatest singular value of matrix G, the H_∞ norm of $G(s)$ can be defined as:

$$\|G\|_\infty \stackrel{\Delta}{=} \sup_{\omega \in \Re} \bar{\sigma}[G(j\omega)] . \tag{28}$$

For a single input-single output system the H_∞ norm of a transfer function can be defined as:

$$\|G\|_\infty = \max_{\omega} \|G(j\omega)\| . \tag{29}$$

The H_∞ optimal control designing problem in the particular case of applying the small gain problem is to form an augmented plant of the process, $P(s)$ like in Fig. 8, with the weighting functions $W_1(s)$, $W_2(s)$, $W_3(s)$ applied to the signals: error e, command u and output y respectively, so that the weighted (y_{11}, y_{12}, y_{13}) and not weighted y_2 system outputs can be defined as:

$$\begin{cases} y_{11} = W_1 e = W_1(u_1 - P_N x_2) = W_1 u_1 - W_1 P_N u_2 \\ y_{12} = W_2 u = W_2 u_2 \\ y_{13} = W_3 y = W_3 P_N u_2 \\ y_2 = e = u_1 - P_N u_2 \end{cases} \tag{30}$$

and the real, perturbed process $P(s)$ can be described as:

$$P(s) = \begin{bmatrix} W_1(s) & -W_1(s)P_N(s) \\ 0 & W_2(s) \\ 0 & W_3(s)P_N(s) \\ I & -P_N(s) \end{bmatrix} . \tag{31}$$

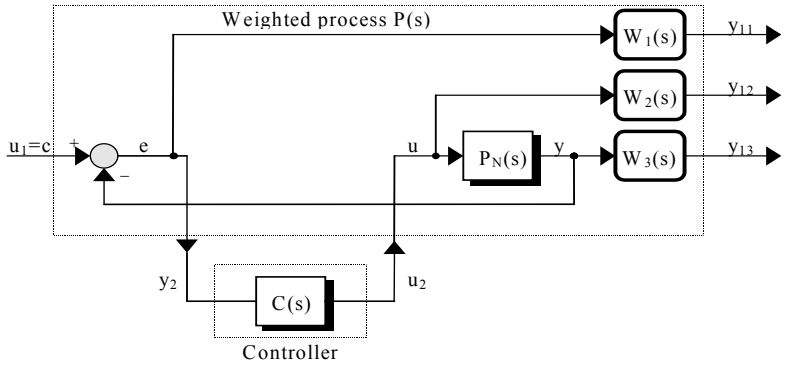

Fig. 8. Structure of speed control system with weighted process.

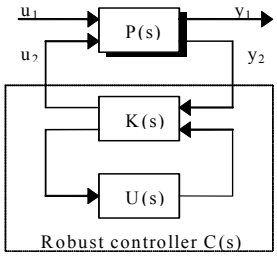

Fig. 9. Robust H_∞ controller

The second step of the robust control designing problem is to find an optimal stabilizing H_∞ controller having the structure presented in Fig. 9. The optimal stabilizing H_∞ controller is described by the control law:

$$u_2(s) = C(s)y_2(s) \tag{32}$$

so that the infinity norm of the cost function T_{y1u1}, defined as:

$$T_{y1u1}(s) \overset{\Delta}{=} \begin{bmatrix} W_1(s)S(s) \\ W_2(s)R(s) \\ W_3(s)T(s) \end{bmatrix} \tag{33}$$

is minimized and is less then one (Doyle et al., 1989; Kwakernaak, 1993):

$$\left\| T_{y1u1} \right\|_\infty < 1\,, \tag{34}$$

where

$$\begin{cases} S(s) = [I + P(s)C(s)]^{-1} \\ R(s) = C(s) \cdot [I + P(s)C(s)]^{-1} = C(s) \cdot S(s) \\ T(s) = P(s)C(s) \cdot [I + P(s)C(s)]^{-1} = I - S(s) \end{cases}. \tag{35}$$

Considering the robust stability and robust performance criteria, the weighting functions for the optimal H_∞ controller are chosen and then the iterative computing process continues, until the norm condition is full fit. The performance design specifications of the speed control loop with the H_∞ controller are imposed in frequency domain (Ionescu et al., 1998; Morari & Zafiriou, 1990):

- robust performance specifications: minimizing the sensitivity function S (reducing it at least 100 times to approximate 0.3333 rad/sec).
- robust stability specifications: -40 dB/decade roll-off and at least -20dB at a crossover band of 100 rad/sec.

According to them, following weighting functions have been considered to describe the perturbed AC drive system with variable moment of inertia and friction coefficient:

$$\begin{cases} \dfrac{1}{W_1(s)} = W_1^{-1}(s) = \dfrac{1}{\gamma} \cdot \dfrac{(3s+1)^2}{100} \\ \dfrac{1}{W_3(s)} = W_3^{-1}(s) = \dfrac{150}{s+145} \end{cases}, \tag{36}$$

where γ represents the actual step value. The iterative process continues, until the graphic representation in Bode diagram of cost function T_{y1u1} reach its maximum value in the proximity of 0 dB axis. In our case, for γ=39,75 we obtain the infinite norm

$$\left\| T_{y1u1} \right\|_\infty = 0,9999 . \tag{37}$$

Respecting condition imposed by Equation 34 the corresponding H_∞ speed controller is:

$$H_\infty(s) = \frac{2327s^2 + 22211s + 16495}{s^3 + 822951s^2 + 548632s + 91442} . \tag{38}$$

The inverse weighting functions $W_1^{-1}(s)$ and $W_3^{-1}(s)$ and the sensitivity functions $S(s)$ and $T(s)$ are presented in Fig. 10. From the diagram results the influence of the weighting function $W_3^{-1}(s)$ to limit the peak value of $T(s)$ function. The output of the speed controller, i.e. the active current component, was limited.

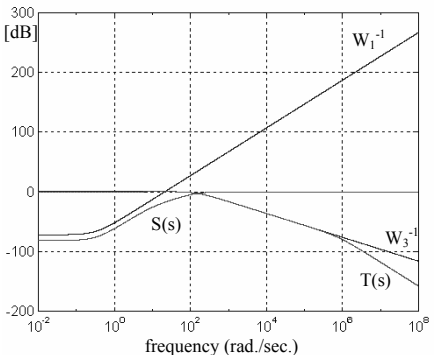

Fig. 10. Weighting functions $W_1^{-1}(s)$, $W_3^{-1}(s)$ and sensitivity functions $S(s)$ and $T(s)$.

The logarithmic Bode diagram and the Nyquist diagram of the direct-loop transfer function of the weighted process are presented in Fig. 11. According to them we establish the following stability parameters: crossover band $\Delta\omega_B$ = 153,7 rad./sec., stability margins: gain margin = 130,3 dB, phase margin = 86,8°. For the same performance and robust stability specifications, a great number of weighting functions described by Equation 36 can be chosen, so the solution of designing an optimal H_∞ controller is not unique (Chiang & Safonov, 1992; Zames, 1996). To analyze if the speed control structure with the H_∞ controller presented in Equation 38 is robust stable, we apply the stability theorem for a perturbation in the drive system, namely a highest variation of total inertia moment from J_{mot} to $10J_{mot}$ and of the friction coefficient B_{mot} to $100*B_{mot}$. The condition

$$\left\| \overline{\Delta_M}(s)T(s) \right\|_\infty < 1 \tag{39}$$

must be tested, where $\overline{\Delta_M}(s)$ represents the greatest multiplicative uncertainty for the nominal plant.

4.2.1 Stability analyze for a variation from J_{mot} to $10J_{mot}$

Considering the calculus way of the transfer function of the process, a ten times growing of the inertial moment, practically means a ten time growing of the time constant of the fixed part. The transfer functions of the nominal process and of the disturbed process are:

$$\begin{cases} P_N(s) = \dfrac{K_m}{T_m s + 1} \\ P(s) = \dfrac{K_m}{10T_m s + 1} \end{cases}, \tag{40}$$

Using Equation 27 and considering T_m=1,232 sec., the maximum multiplicative uncertainty in the case of ten times growing the inertial moment J, can be modeled:

$$\overline{\Delta_M}(s) = \frac{-9T_m s}{10T_m s + 1} = \frac{-11,097s}{12,33s + 1} \tag{41}$$

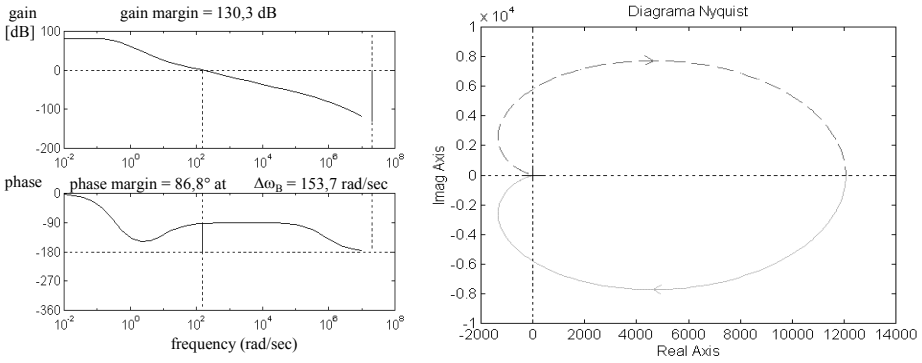

Fig. 11. Direct-loop transfer function of the weighted process in Bode and Nyquist diagram.

Knowing the expression of the complementary sensibility function T(s), the condition of robust stability can be determined, and is:

$$\left\| \overline{\Delta_M}(s)T(s) \right\|_\infty = 0,9359 . \tag{42}$$

Concluding, the control system with H_∞ controller remains robust stable for a variation of 10 times of the total inertial moment of the system, related to the catalogue one. Fig. 12 shows the direct-loop transfer function $H_d(s)$ family curves for the PI controller and for the optimal $H_{\infty,}$ controller, at variations of the inertial moment of the synchronous motor, starting at J_{mot} value, from 3, 5, 7 and 10 times of this value. As we can see from the presented graphs, at the variations of J, though the PI controller doesn't go in instability, thus it is more sensitive at the parameter variations than the H_∞ controller. This shows a better robustness of the H_∞ optimal regulator.

4.2.2 Stability analyze for a variation from B_{mot} to $100B_{mot}$

Considering that the largest variation of the friction coefficient of the mechanical system is $100*B_{mot}$ catalogue value. A greater friction coefficient practically means a smaller value of the time constant as like of the amplification factor of the fixed part. Considering the above mentioned, the transfer functions of the nominal process and of the disturbed processes are:

$$\begin{cases} P_N(s) = \dfrac{K_m}{T_m s + 1} \\ P(s) = \dfrac{K_m / 100}{(T_m / 100)s + 1} \end{cases} . \tag{43}$$

Using Equation 27 and the time constant of the nominal process, the maximal multiplicative uncertainty, in the case of $100*B_{mot}$ friction coefficient, can be written as:

$$\overline{\Delta_M}(s) = \frac{-99}{T_m s + 100} = \frac{-99}{1,232s + 100} . \tag{44}$$

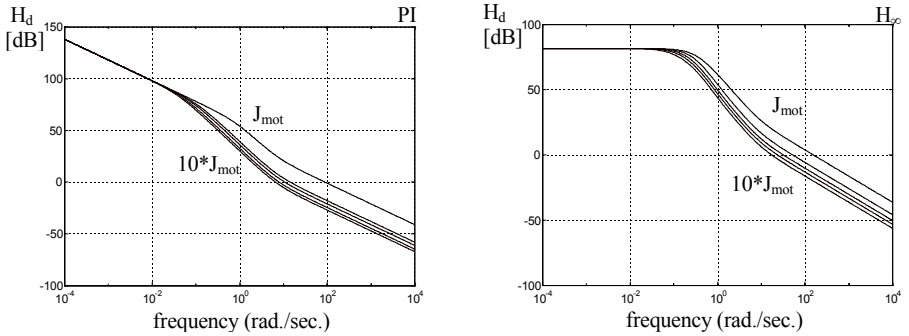

Fig. 12. Bode diagram of direct-loop transfer functions for PI (left) and H_∞ controller (right), at different inertia moment values.

The robust stability condition will be expressed as:

$$\left\| \overline{\Delta_M}(s)T(s) \right\|_\infty = 0,9999 . \tag{45}$$

We can find that the control system with the H_∞ controller remains robust stable for a 100 times variation of the friction coefficient.

5. Simulated and experimental results

Some results of the sensorless control of AC machines based on adaptive identification are presented in main paragraph 3. Because of its sensitivity to parameter variations and external perturbations, a robust solution for the speed controller was proposed and discussed in paragraph 4. Simulated results of an AC drive system controlled by a robust optimal H_∞ controller (chapter 5.1) will demonstrate the advantage of using robust control in applications with permanent variation of system parameter or external perturbations, (i.e. robot arms, traction systems, etc.). Finally, some experimental results of a robust control system, with sensorless AC drive, based on adaptive identification, will be presented.

5.1 Simulated results of robust controlled driving system with permanent magnet synchronous machine

A variable speed, FOC structure, of the PM-SM with cancelled longitudinal reaction, fed by a PWM voltage source inverter is presented in Fig.13. The stator current vector split into components leads to the characteristic loops of a FOC system. Rotor position information is obtained from the encoder and rotor speed is computed. The control system was simulated in Matlab/Simulink. The speed controller was designed and simulated using more optimizations criteria, to be compared with. The designed optimal robust H_∞ controller was implemented (see Equation 33), a PI controller (see Equation 6) and an optimal H_2 controller based on the same performance design specifications like the optimal robust H_∞ controller.

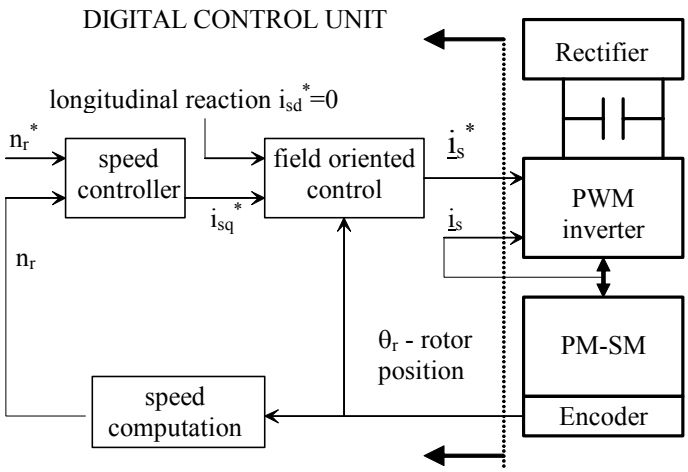

Fig. 13. Variable speed VC structure of PM-SM with different types of speed controller.

The power converter is a 1kW voltage source converter, composed by a diode rectifier and a PWM inverter. The PM-SM is a three phase machine, having following catalog values:

- rated speed n_N 3000 rev/min,
- rated torque M_N 1,7 Nm,
- electromotive constant k_E 110 V/(1000 rpm.),
- rated power P_N 530 W,
- motor constant k_M 1,05 Nm/A,
- magnetic induction B 1,3 T,
- rated stator current I_N 1,6 A,
- pole pairs z_p 3,
- PM flux Ψ_{PM} 0,2334 Wb,
- d ax stator inductance L_{sd} 0,049 H,
- q ax stator inductance L_{sq} 0,046 H,
- stator resistence R_s 10 Ω,
- inertia moment J_{mot} $1{,}85*10^{-4}$ kgm^2,
- friction coefficient B_{mot} $5*10^{-5}$ Nm(rad/sec)$^{-1}$.

Fig. 14 presents the simulated results for a speed control of the synchronous machine with the designed PI, H_2, and H_∞ controller, having all parameters at the nominal value, for a starting process to the rated rotor speed with no load torque (left diagram) and with rated load torque (right diagram). In Fig. 15 the speed response is for a perturbed plant with total friction coefficient $B_{tot}=50B_{mot}$ for the same imposed speed step without (left) and with nominal load torque (right). The speed response for a similar simulation of a perturbed plant with total moment of inertia variation $J_{tot}=11J_{mot}$ is presented in Fig. 16 for a no load start (left) and a rated load start (right).

For the nominal plant the dynamic performances at a speed step are similar for all three controllers. It is normal to be so, because the controllers have been designed using a simplified model of the machine, working in the steady-state nominal point. The advantage of using optimal H_∞ robust controller is evident in the presented simulations when the nominal plant is perturbed, by changing the load torque, the total moment of inertia or the friction coefficient.

Fig. 17 presents the speed response for a speed control of the synchronous machine with the designed PI, H_2, and H_∞ controllers for a starting process at rated speed with no load followed at 0.3 sec. by a rated load step (1.7 Nm). Fig. 18 details the imposed torque step m_r and the obtained electromagnetic torque m_e and dynamic torque m_j. A starting process at rated speed, followed by a stopping process for the PM-SM without load and with rated load is presented in Fig. 19. A simulation of the starting process with low speed step is also presented in Fig. 20 for all three types of designed controllers.

In conclusion, we consider that the H_∞ optimal robust controller ensures good dynamical performances and stability for a domain of variation large enough of the parameters that can be modified in the process. In applications, where electromechanical parameter variations or load perturbations appear (such as robot control), performant drive systems with AC machines can be considered, by using robust speed (or position) controllers.

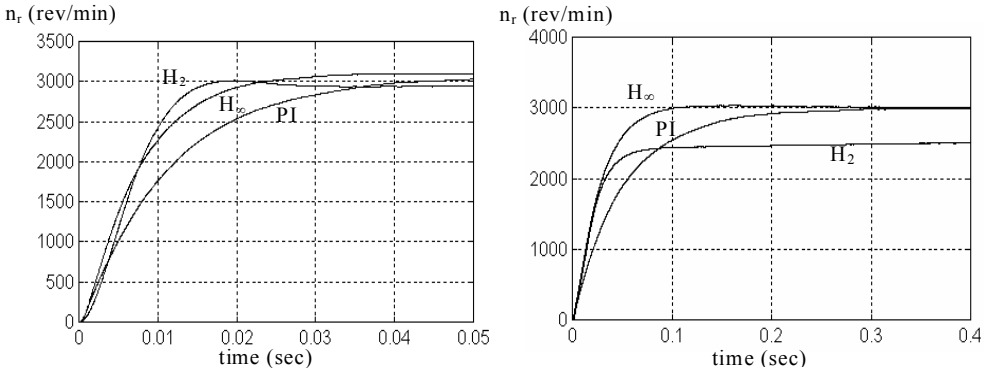

Fig. 14. Starting process with PI, H_2 and H_∞ controller for a nominal plant without load torque (left) and with rated torque (right).

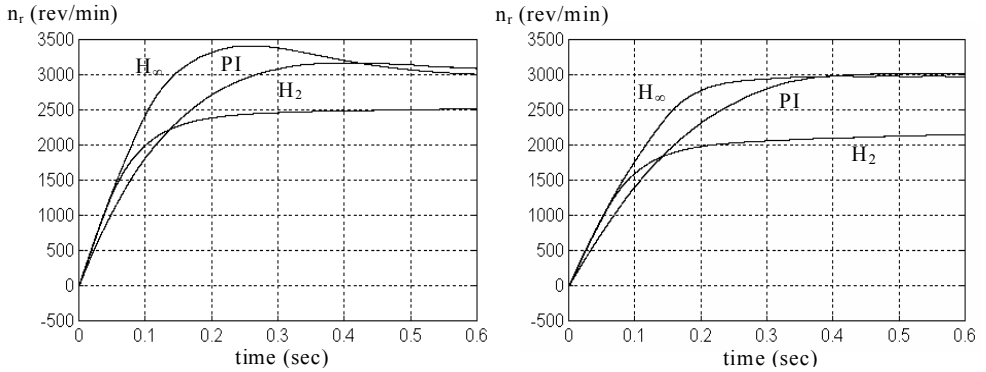

Fig. 15. Starting process with PI, H_2 and H_∞ controller for a perturbed plant (moment of inertia $J_{tot}=11J_{mot}$) without load torque (left) and with rated torque (right).

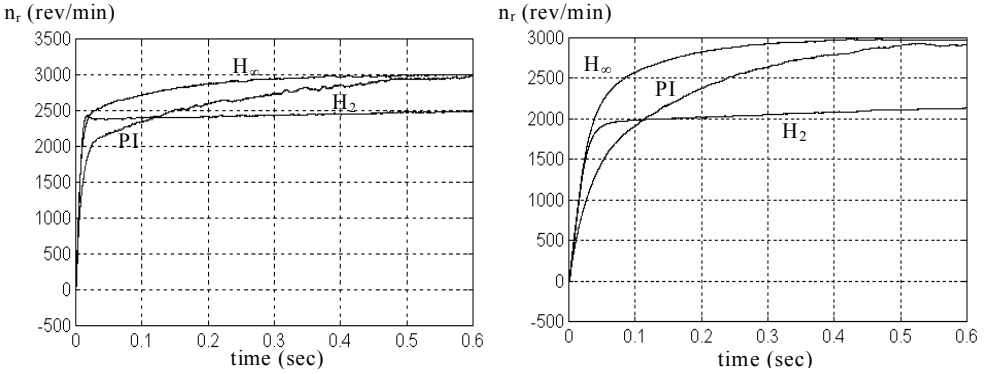

Fig. 16. Starting process with PI, H_2 and H_∞ controller for a perturbed plant (friction coefficient $B=50B_{mot}$) without load torque (left) and with rated torque (right).

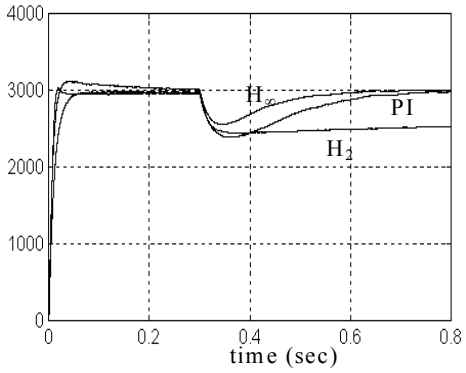

Fig. 17. Speed response for speed and torque steps

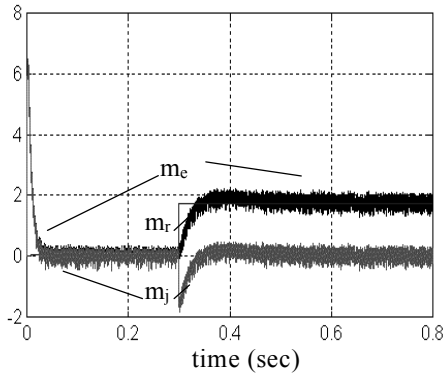

Fig. 18. Torque diagrams.

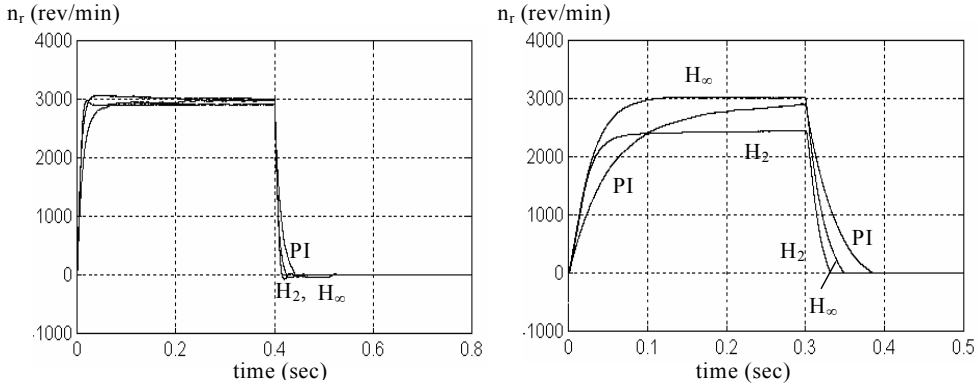

Fig. 19. Starting and fast stopping process with PI, H_2 and H_∞ controllers for a nominal plant with no load (left) and with rated load (right).

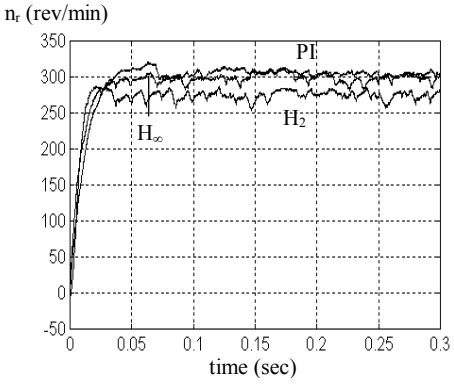

Fig. 20. Speed response at low speed step (300 rev/min) with PI, H_2 and H_∞ controllers.

5.2 Experimental results of robust controlled sensorless driving system with induction machine and adaptive speed estimation

The control unit is based on the fixed-point TMS320C50 Digital Motor Control Board developed by Texas Instruments. The complete schematic of the control architecture is presented in Fig. 21. It is composed of:

- a high speed TDM type serial bus for interconnection with the master processor and with the other dedicated processors.
- the control board (target hardware) consisting in a microcomputer, based on the TMS320C5x signal processor and the following dedicated modules:
- a PWM unit controlled by the processor and realized in FPGA technologies, which generates the three output signals for the power converter;
- a interfacing unit to the incremental encoder giving the position of the rotor (used to confirm the speed estimation algorithm), also implemented in FPGA technologies;
- an analogic signal acquisition unit consisting in a A/D converter and an analogic multiplexer for 8 channels, used for the input of the stator currents and voltages.
- the AC drive system composed by a frequency voltage source PWM converter with current reaction and a induction machine having following main parameters:
- rated power P_N 2,2 *kW*,
- rated speed n_N 1435 rpm.,
- nominal stator current I_{sN} 4,9 *A*,
- rated stator voltage U_{sN} 400*V*,
- nominal load torque M_N 14,7 *Nm*.
- a debugging computer interfaced to the target hardware through a serial RS232 driver and an emulation and debugging module XDS510. This computer will be used only in the software developing and debugging phase.

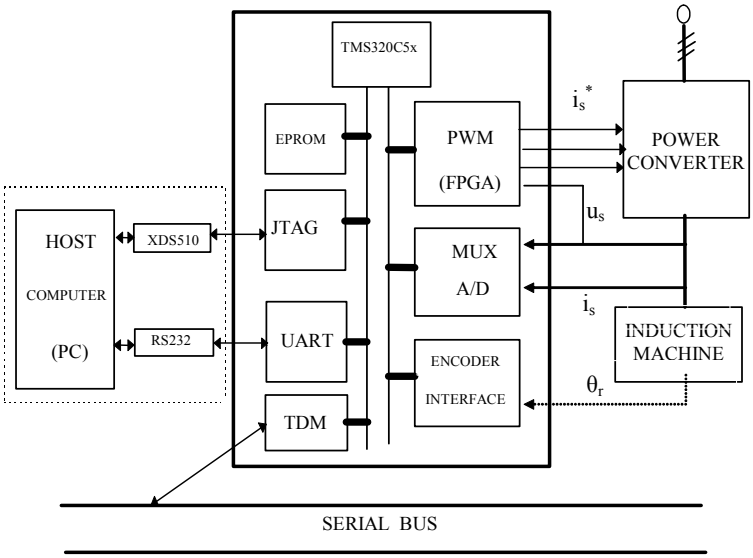

Fig. 21. Hardware structure of the robust controlled sensorless driving system with induction machine and adaptive speed estimation.

The three control loops (presented also in Fig. 13), namely: speed control loop, implemented with a robust controller; minor loop, necessary for the field-orientation based on the rotor flux and the stator current control loop of the PWM generator are software implemented. In order to obtain the best approach speed and accuracy a fixed point, fractional arithmetic was used. The program modules are: *main*( ) the main loop realizing the hardware initialization and the communication functions with the main processor and the other dedicated processors; *tint*( ) interrupt handling routine executing the current control loop and minor control loop and *int_4*( ) interrupt handling routine executing the PWM current control loop. The TMS320C5x assembler language was used to achieve an effective software implementation for the *main* routine and ANSI-C language was used for the control routines *tint* and *int_4*. Library functions (in C or assembly language) are used for handling the incremental encoder, the A/D converter, the PWM control signal generator and the communication through the serial interface with the screen terminal. The interrupts are generated by programmable counters. So *tint* interrupt is generated by processor internal programmable counter and has a 100μs period. *Int_4* interrupt is generated by the PWM module and has a 10μs period.

The dynamic evolution of rotor speed, estimated speed based on the MRAS algorithm and speed error for a robust controlled (using the optimal H_∞ controller) starting process of the sensorless driving system with induction machine at rated speed step with no load torque is presented in Fig. 22. It can be observed, that the maximum speed error in the dynamic process (starting process) is less then 9 rpm, that means a relative error (speed error/real speed) of around 0,6%, which is a considerable better value then the results obtained for the same sensorless drive system, without a robust speed controller. The relative sped error of the sensorless robust control, after the transitory dynamic process is ended and the drive system works at stabilized speed, is less then 0.05%, which means a really performant estimation (less then 0,7 rpm.). The differences between the two sensorless control structures, the one without a robust control (speed control results presented in Fig.6) and the one with robust control (speed control results presented in Fig. 22), can be explained by the increased robustness imposed by the optimal H_∞ controller, to a process (the AC drive system) which is sensitive to parameter variations (rotor time constant) and external perturbations (moment of inertia, friction coefficient), because of the adaptive estimation algorithm used to determine the rotor speed.

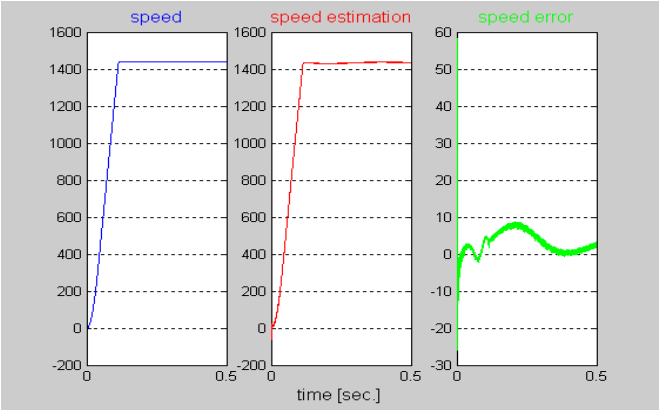

Fig. 22. Speed, estimated speed and speed error for a robust controlled starting process.

The speed and estimation speed error for the same control structure at a full loaded starting process (with nominal imposed torque) are presented in Fig. 23. The time constant of the transitory starting process is as expected a few times bigger than in the starting process with no load (Fig.22.) and the relative speed error is around 0,3%, that means less then at no-load start. That can be explained, due to the fact that the speed estimator itself is less sensitive to parameter variations when it works with nominal inputs. The dynamic evolution of the different currents of the induction machine for the same process are presented in Fig. 24, namely the stator current, the active (torque producing) and reactive (flux producing) components of the stator current and the estimated magnetizing current.

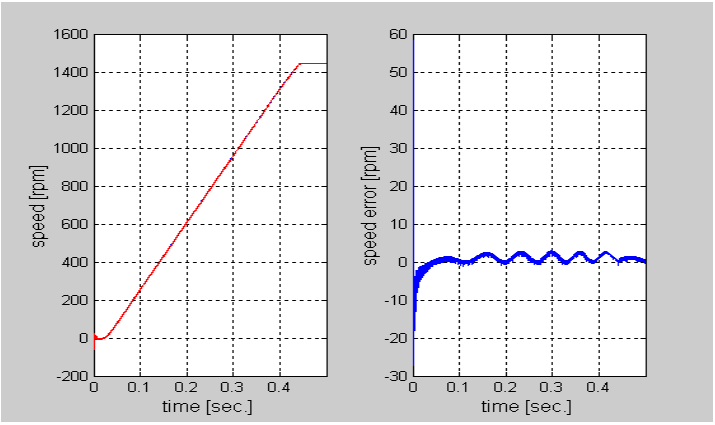

Fig. 23. Rotor speed and speed error at rated load starting process.

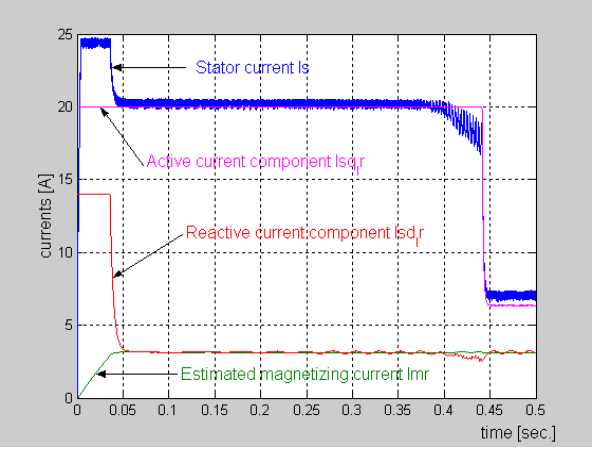

Fig. 24. Different currents of the IM at a starting process with rated load.

The dynamic behavior of the AC drive, if a rated load step is imposed to the system running at a stable rotor speed (rated speed), is tested. Fig. 25 presents the performance indexes of the MRAS based speed identification algorithm (the reference model performance index p,

the adjustable model performance index $\hat{p}$, and the error ε), the imposed load torque step at 0,31 sec. and the developed electromagnetic torque of the AC machine. The stator current was limited in the starting process to a 3,5 times value of the rated current ($I_{s,max}$=17A). The estimated speed, the rotor speed and the speed error are presented in Fig. 26. The maximum relative speed error in the transitory process (around 1,4%), is significantly greater as for a rated speed step and the zero convergence time of the speed error is significantly longer. It is an expected result because in all presented FOC structures, by using a speed controller in the active control loop of the AC drive (Fig. 2 and Fig. 13), the rotor speed is directly controlled while the electromagnetic torque is indirectly controlled. In applications where a direct torque control is needed, the dynamic performances of torque response can be improved.

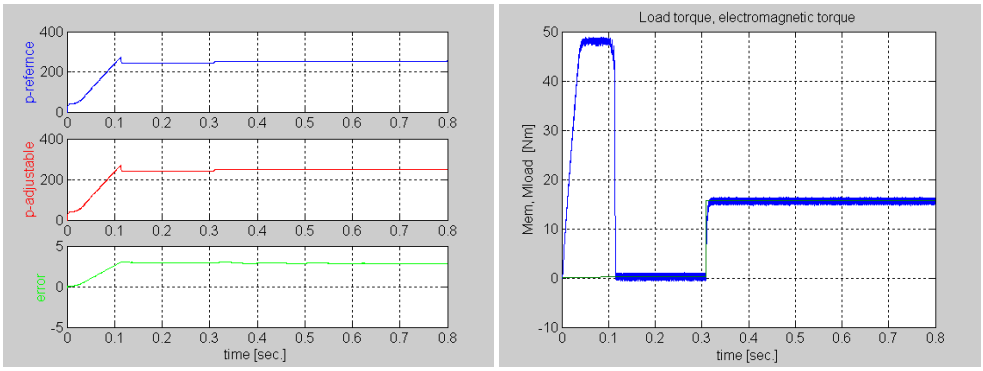

Fig. 25. Performance indexes of MRAS algorithm (left diagram), imposed load torque step and developed electromagnetic torque (right diagram).

Fig. 26. Speed evolution for a starting process and a rated load step at t=0.3 sec.

The results confirm, that the robust control, using an optimal H_∞ speed controller, of the sensorless AC drives, based on adaptive identification with MRAS algorithm for speed estimation, assure:

- good estimation in steady state and transient operations;
- robustness to electrical parameter variations as stator resistance and mutual inductance (reference model) or rotor time constant (adjustable model);
- robustness to external perturbations (moment of inertia, friction coefficient),

but needs greater computing time for the control loop, that means more powerful real time computing systems (with high frequency digital signal processors) and increasing costs.

6. Conclusion

Sensorless control of AC drive systems became in the last years a challenge for intelligent motion control. To estimate rotor speed or position, by using adaptive identification algorithms based on model reference, is a relative easy task and became therefore a valuable solution for applications where not high precision of speed/position estimation is needed. The main disadvantage of the MRAS identification algorithms is the relative high sensitivity to machine parameter variations (i.e. rotor time constant) and to external perturbations (i.e. moment of inertia, friction coefficient). Using the robust control theory seams to be a good solution to increase the speed/position estimation accuracy and to apply the same estimation method for a large number of motion control applications. The optimal H_∞ speed controller makes the AC drive system stable to a large scale of parameter variations and perturbations and provides high dynamic performance as well as accurate speed estimation to the sensorless control structure.

7. Acknowledgment

The author would like to acknowledge the Alexander von Humboldt Foundation for their support in the research activity, which made possible an important part of the presented results.

8. References

Akatsu, K. & Kawamura, A. (2000). Sensorless Very Low-Speed and Zero-Speed Estimation with Online Rotor Resistance Estimation of Induction Motor Without Signal Injection. In *IEEE Transactions on Industry Applications*, Vol.36, No.3, pp.764-771, ISSN: 0093-9994

Akpolat, H., Asher, G. & Clare, J. (2000). A Practical Approach to the Design of Robust Speed Controllers for Machine Drives. In *IEEE Transactions on Industrial Electronics*, Vol.47, No.2, pp. 315-324, ISSN: 0278-0046

Apkarian, P., Morris, J. (1993). Robust modal controllers. New H_∞/μ synthesis structures. In *Proceedings of the European Control Conference ECC'93*, Groningen, Netherlands, March 1-4, 2003, pp. 1819-1825

Ball, J., Helton, J. (1993). Nonlinear H_∞ Control Theory: A Literature Survey. In *Automatica*, Vol. 29, No. 2, Great Britain, pp. 1-12, ISSN: 0005-1098

Birou, I. & Pavel, S. (2008). Sensorless AC Driving Systems Based on Adaptive Identification Algorithms and Robust Control Strategies. In *Proceedings of the 9th International Conference DAS'2008,* May 22-24, Suceava, Romania, pp. 93-96, ISSN 1844-5038

Birou, I., Maier, V., Pavel, S. & Rusu, C. (2010). Control of AC Drives; a Balance Between Dynamic Performance, Energy Efficiency and Cost Constrains. In: *Anals of University of Craiova, Electrical Engineering series,* No. 34, Vol. II, Craiova, Romania, 7-8 oct. 2010, pp. 42-47, ISSN 1842-4805

Briz, F., Degner, M., Garcia, P. & Lorenz, R (2004). Comparison of Saliency–Based Sensorless Control for AC Machines. In *IEEE Transactions on Industry Applications*, Vol.40, No.4, pp. 1107-1115, ISSN: 0093-9994

Bryson, A. (1996). Optimal control. In *IEEE Control Systems*, Vol. 16, No.3, pp. 26-33

Caruana, C., Asher, G., Bradley, K. & Woolfson, M. (2003). Flux Positon Estimation in Cage Induction Machines Using Synchronous HF injection and Kalman Filtering. In *IEEE Transactions on Industry Applications*, Vol.39, No.5, pp. 1372-1378, ISSN: 0093-9994

Chiang, R. & Safonov, M. (1992). *Robust Control Toolbox. User's Guide*. The Math Works Inc., Massachusetts, 1992

Cirrincione, M. & Pucci, M. (2005). An MRAS-Based Sensorless High-Performance Induction Motor Drive With a Predictive Adaptive Model. In *IEEE Transactions on Industrial Electronics*, Vol.52, No.2, pp. 532-551, ISSN: 0278-0046

Consoli, A., Scarcella, G., Testa, A. (2003). Using the Induction Motor as Flux Sensor: New Control Perspectives for Zero-Speed Operation of Standard Drives. In *IEEE Transactions on Industry Electronics*, Vol.50, No.5, pp.1052-1061, ISSN: 0278-0046

Degner, M. & Lorentz, R. (2000). Position Estimation in Induction Machines Utiliying Rotor Bar Slot Harmonics and Carrier–Frequency Signal Injection. In *IEEE Transactions on Industry Applications*, Vol.36, No.3, pp.736-742, ISSN: 0093-9994

Doyle, J., Glover, K., Khargonekar, P. & Francis, B. (1989). State space solutions to standard H_2 and H_∞ control problems. In *IEEE Transaction on Automatic Control*, Vol.34, pp. 831-847

Green, M. & Limebeer, D. (1995) *Linear Robust Control*. Prentice-Hall, Englewood Cliffs, 1995

Hinkkanen, M. (2004) Analysis and Design of Full-Order Flux Observers for Sensorless Induction Motors. In *IEEE Transactions on Industrial Electronics*, Vol.51, No.5, pp. 1033-1040, ISSN: 0278-0046

Holtz, J. & Quan, J. (2002). Sensorless Vector Control of Induction Motors at Very Low Speed Using a Nonlinear Inverter Model and Parameter Identification. In *IEEE Transaction on Industry Applications*, Vol.38, No.4, pp.1087-1095, ISSN: 0093-9994

Holtz, J. (2002). Sensorless control of induction motor drives. In *Proceedings of the IEEE*, vol. 90, No. 8, August 2002, pp. 1359-1368, ISSN: 0018-9219

Holtz J. (2006). Sensorless Control of Induction Machines – with or without Signal Injection?. In *IEEE Transactions on Industrial Electronics*, Vol.53, No.1, pp. 7-30, ISSN: 0278-0046

Hurst, K., Habetler, T., Griva, G. & Profumo, F. (1998). Zero-speed tacholess induction machine torque control: simply a meter of stator voltage integration. In *IEEE Transactions on Industrial Applications*, Vol. 34, No.4, pp. 790-795, ISSN: 0093-9994

Ionescu, V., Oara, C. & Weiss, M. (1998). *Generalized Ricatti Theory and Robust Control: A Popov Function Approach*, John Wiley & Sons Ltd., Chichester, New York, 1998

Jansen, P., Lorenz, R. & Novotny, D. (1994). Observer-Based Direct Field Orientation: Analysis and comparison of alternative methods. In *IEEE Transactions on Industrial Applications*, Vol. 30, No.4, pp. 945-953, ISSN: 0093-9994

Kelemen, A. & Imecs, M. (1991) *Vector Control of AC Drives. Vol.1: Vector Control of Induction Machine Drives*. Omikk Publisher, Budapest, 1991

Kim, H., Lorenz, R. (2004). Carrier Signal Injection based Sensorless Control Methods for IPM Synchronous Machine Drives. In *Proceedings of the 39th IEEE-IAS Annual Meeting*. Vol. 2, pp. 977-984, ISBN: 0-7803-8486-5

Kucera, V. (1993). The LQG and H_2 Designs: Two Different Pproblems?. In *Proceedings of the European Control Conference*, Groningen, Netherlands, March 1-4, 2003, pp. 334-337.

Kwakernaak, H. (1993). Robust Control and H_∞ - Optimization. Tutorial Paper. In *Automatica,* Vol. 29, No. 2, pp. 255-273, ISSN: 0005-1098

Landau, I. (1979). *Adaptive Control-The Model Reference Approach*, Marcel Dekker, New York

Lascu, C., Boldea, I., Blaabjerg, F. (2005). Very-Low-Speed Variable-Structure Control of Sensorless Induction Machine Drives Without Signal Injection. In *IEEE Transactions on Industrial Applications*, Vol. 41, No.2, pp. 591-598, ISSN: 0093-9994

Leonhard, W. (1985). *Control of Electrical Drives*. Springer-Verlag, Berlin, 1985

Lorenz, R., (2010). Core Sensor Integration Technologies for Advanced Electrical Drives and Power Converters-Keynote Speaker, In *Proc. of Int. Conference on Development and Application Systems DAS'2010,* May 27-29, 2010, Suceava, Romania, ISSN 1844-5020

McFarlane, D., Glover, K. (1990). Robust Controller Design Using Normalized Coprime Factor Plant Descriptions. In *Lecture Notes in Control and Information Sciences*. Springer-Verlag, Berlin, Heidelberg, New York, 1990

Mita, T., Hirata, M., Murata, K. & Zhang, H. (1998). H_∞ Control Versus Disturbance-Observer-Based Control. In *IEEE Transactions on Industrial Electronics*, Vol.45, No.3, pp. 488-495, ISSN: 0278-0046

Morari, M., Zafiriou, E. (1990). *Robust Process Control*, Prentice Hall, Englewood Cliffs, 1990

Moreira, J., Hung, K., Lipo, T. & Lorenz, R. (1991). A simple and robust adaptive controller for detuning correction in field oriented induction machines. In *Proceedings of IEEE-IAS Annual Meeting*, pp.397-403, ISBN: 0-7803-0453-5

Rajashekara, K., Kawamura, A. & Matsuse, K. (1996). *Sensorless Control of AC Motor Drives*. IEEE Press, Piscataway, New Jersey, 1996

Safonov, M. (1980). *Stability and Robustness of Multivariable Feedback Systems*. MIT Press, 1980

Toliyat, H., Levi, E. & Raina, M. (2003). A Review of RFO Induction Motor Parameter Estimation Techniques. In *IEEE Transactions on Energy Conversion*, Vol. 18., No.2, pp. 271-283, ISSN: 0885-8969

Trzynadlowski, A. (1994). *The Field Orientation Principle in Control of Induction Motors*. Kluwer Academic Publishers, Boston, 1994

Vas, P. (1998). *Sensorless Vector and Direct Torque Control*, Oxford University Press, 1998

Wieser, R. (1998). Optimal rotor flux regulation for fast-accelerating induction machines in the field-weakening region. *IEEE Transactions on Industry Applications*, Vol.34, No.5, pp. 1081-1087, ISSN: 0093-9994

Zadeh, L. (1996). The evolution of systems analysis and control: a personal perspective. In *IEEE Control Systems*, Vol. 16, No.3, June 1996, pp. 95-98

Zames, G. (1996). Input-output feedback stability and robustness. In *IEEE Control Systems*, Vol. 16, No.3, June 1996, pp. 61-66

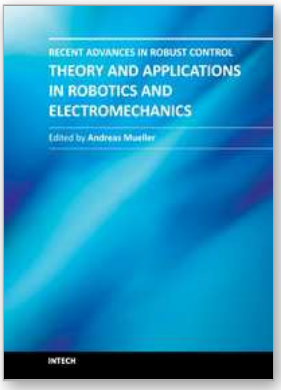

Recent Advances in Robust Control - Theory and Applications in Robotics and Electromechanics

Edited by Dr. Andreas Mueller

ISBN 978-953-307-421-4
Hard cover, 396 pages
Publisher InTech
Published online 21, November, 2011
Published in print edition November, 2011

Robust control has been a topic of active research in the last three decades culminating in H_2/H_\infty and \mu design methods followed by research on parametric robustness, initially motivated by Kharitonov's theorem, the extension to non-linear time delay systems, and other more recent methods. The two volumes of Recent Advances in Robust Control give a selective overview of recent theoretical developments and present selected application examples. The volumes comprise 39 contributions covering various theoretical aspects as well as different application areas. The first volume covers selected problems in the theory of robust control and its application to robotic and electromechanical systems. The second volume is dedicated to special topics in robust control and problem specific solutions. Recent Advances in Robust Control will be a valuable reference for those interested in the recent theoretical advances and for researchers working in the broad field of robotics and mechatronics.

How to reference

In order to correctly reference this scholarly work, feel free to copy and paste the following:

Birou M.T. Iulian (2011). Robust Control of Sensorless AC Drives Based on Adaptive Identification, Recent Advances in Robust Control - Theory and Applications in Robotics and Electromechanics, Dr. Andreas Mueller (Ed.), ISBN: 978-953-307-421-4, InTech, Available from: http://www.intechopen.com/books/recent-advances-in-robust-control-theory-and-applications-in-robotics-and-electromechanics/robust-control-of-sensorless-ac-drives-based-on-adaptive-identification

INTECH
open science | open minds

InTech Europe
University Campus STeP Ri
Slavka Krautzeka 83/A
51000 Rijeka, Croatia
Phone: +385 (51) 770 447
Fax: +385 (51) 686 166
www.intechopen.com

InTech China
Unit 405, Office Block, Hotel Equatorial Shanghai
No.65, Yan An Road (West), Shanghai, 200040, China
中国上海市延安西路65号上海国际贵都大饭店办公楼405单元
Phone: +86-21-62489820
Fax: +86-21-62489821